Available online at www.sciencedirect.com

ScienceDirect

Procedia Materials Science 3 (2014) 894 – 899

Procedia Materials Science

www.elsevier.com/locate/procedia

20th European Conference on Fracture (ECF20)

Influence of inclusion type on internal fatigue fracture under cyclic shear stress

Yusuke Sandaiji*, Eiichi Tamura, Takehiro Tsuchida

Kobe Steel Ltd., Materials Research Laboratory, 1-5-5 Takatsukadai, Nishi-ku, Kobe, Hyogo, Japan

Abstract

Four kinds of high carbon chromium steel were conducted to ultrasonic torsional fatigue test and the fracture surfaces and the cross-sections of fracture origin were observed. Internal fatigue fracture was occurred from oxide inclusion and MnS, and ODA was found surrounding inclusion. The behaviors of the crack initiation and propagation were different depending on inclusion types. Thus the characteristics of inclusion influence to fatigue properties.

Selection and peer-review under responsibility of the Norwegian University of Science and Technology (NTNU), Department of Structural Engineering

Keywords: Very high cycle fatigue; Torsional loading; Inclusion-initiated fracture; Bearing steel; Ultrasonic fatigue test

1. Introduction

In the very high cycle fatigue regime (VHCF) beyond 10^7cycles, a fatigue crack initiates from internal non-metallic inclusion in high strength steel and so many studies have been done to clarify the mechanism [1] - [6]. In the VHCF, a characteristic fracture surface, which is named “optically dark area (ODA)” [1] etc. [5] [6], is found surrounding fracture origin and the most of fatigue life is spent to form it [7]. But the mechanisms of internal crack propagation and characteristic fracture surface formation are not yet well understood. Because the fracture origin is inclusion, it is supposed that the fatigue properties of the inclusion-initiated fracture were affected by inclusion size and type. Furuya et al. [8] reported that there is significantly difference of fatigue life due to inclusion types.

* Corresponding author. Tel.: +81-78-992-5503; fax:;81-78-992-5512.
E-mail address: sandaiji.yusuke@kobelco.com

Selection and peer-review under responsibility of the Norwegian University of Science and Technology (NTNU), Department of Structural Engineering
doi:10.1016/j.mspro.2014.06.145

Some part of bearings, such as ball or ring, is applied cyclic shear stress and internal fracture happens in the VHCF, so it is necessary to clarify the mechanism of internal fatigue fracture under cyclic shear stress. However it is difficult to observe the fracture origin with conventional rolling contact test, because the origin is damaged by compression stress. Recently, torsional load type ultrasonic fatigue machine which could apply the shear stress was developed [9] – [11] and the study of torsional fatigue properties in VHCF has been started [12]. Xue et al. [10] performed ultrasonic axial fatigue test and ultrasonic torsional fatigue test to the same high strength steel and found that the type of inclusion at fracture origin is different, the axial load type is $CaO\text{-}Al_2O_3$ and the torsional load type is MnS. This result may means that the influence of inclusion types is different on the load types.

In this research, several bearing steels which contain a variety of inclusions were conducted to ultrasonic torsional fatigue test and fracture surfaces and the cross-sections of fracture origin were observed. The influence of inclusion types were discussed from the crack initiation and propagation behavior.

2. Experimental procedure

2.1. Material and specimen

Four kinds of high carbon chromium steel were used in this study. The chemical compositions are summarized in Table 1. Steel A is commercial bearing steel JIS-SUJ2 and Steel B ~ D were made in laboratory. The chemical compositions of steel B, C and D were controlled to fracture from oxide inclusion, MnS and TiN respectively, so steel B is low S and low Ti content, steel C is high Mn and S content, steel D is high Ti and N content. Each material was spheroidized and rough-machined, then heat-treated as follows; oil quenching from 1123K for 20 minutes, tempering at 438K for 150 minutes. After heat treatment, the materials were machined to the specimen shape shown in Fig. 1. The microstructure is martensite structure and the Vickers hardness is 721, 740, 704 and 698 to steel A ~ D respectively. Some kind of inclusion were found on mirror-polished surface, oxide inclusion in steel A, oxide inclusion and MnS in steel B, MnS in steel C and TiN in steel D. The maximum inclusion sizes in the specimen $\sqrt{area}_{inc,\ max}$ were estimated by extreme value statistic method with the longitudinal sections observation. $\sqrt{area}_{inc,\ max}$ was 11~15μm in steel A, B and D, and 35μm in steel C. Every specimen was added compression residual stress by shot peening to prevent surface-initiated fracture. The compressive residual stress in 45 degrees direction of the specimen axis was measured by X-ray diffraction from surface to 200μm depth with electro-polishing. The compressive residual stress at surface was 511MPa and increased to 1215MPa at 20μm depth, and then decreased to 370MPa at 200μm depth.

Table 1. Chemical compositions (mass %)

Steels	C	Si	Mn	S	Cr	Ti	Al	N	O	Fe
A	0.99	0.26	0.38	0.001	1.44	0.003	0.025	0.007	0.0009	rest
B	1.17	0.30	0.39	0.004	1.45	<0.001	0.014	0.001	0.0012	rest
C	1.06	0.25	0.52	0.099	1.48	<0.001	0.023	0.001	0.0013	rest
D	1.05	0.25	0.37	0.005	1.47	0.053	0.026	0.021	0.0013	rest

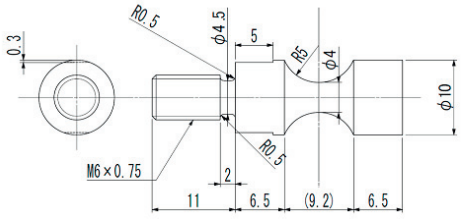

Fig. 1 Shape of the specimen.

2.2. Experimental method

Fatigue tests were conducted by ultrasonic torsional fatigue test machine (Shimadu USF-2000T) under fully reversed torsional loading conditions and the frequency was 20 kHz. The specimens were cooled with compressive dry air during testing. Cyclic loads were applied continuously to steel A and intermittently to steel B ~ D. The fracture surfaces were observed by scanning electron microscope (SEM) and optical microscope. When an inclusion was found at fracture origin, the kind of inclusion was identified by energy dispersive X-ray spectroscopy (EDX). Some cross sections of fracture surface were bared by grinding and observed by SEM.

3. Experimental results

3.1. Fatigue test results

Fig. 2 shows the S-N curves of ultrasonic torsional fatigue test, where the solid symbols means internal fracture and open ones means surface fracture. Both internal fracture and surface fracture were occurred in each steel, and the definite difference on fatigue life was not found with fracture types. The result of fracture surface observation, an inclusion was found at every fracture origin of internal fracture surface. Comparing fatigue life, the fatigue life of steel C is less than the others. The locations of the fracture origins were concentrated between 200 ~ 400μm from specimen surface. Due to the residual compressive stress by the shot-peening, the fracture from surface or sub-surface was prevented and the internal fracture was occurred.

3.2. Fracture surface observation

Fig. 3 (a) shows the overview of the internal fracture surface. The fracture surface was formed an angle of 45 degrees to the specimen axis, therefore the fatigue crack propagated on the plane of the maximum principal stress. From here, the observation was done from the vertical direction to the fracture surface (i. e. from the direction of 45 degrees to the specimen axis). The fracture surface of steel A was shown in Fig. 3 (b). The crack initiated from an internal inclusion and propagated radially. Fig. 4 shows the fracture origins of steel A and steel C. By SEM-EDX analysis, the inclusions were $CaO\text{-}Al_2O_3$ complex inclusion in steel A, MnS in steel B and C, $TiN\text{-}Al_2O_3$ complex inclusion in steel D. The inclusion sizes $\sqrt{area}_{inc}$ that observed at fracture origin were about 10 ~ 20μm in every specimen. Except for steel C, $\sqrt{area}_{inc}$ were almost of the same size to the maximum inclusion size $\sqrt{area}_{inc,\,max}$ which was estimated by extreme value statistic But $\sqrt{area}_{inc}$ was smaller than $\sqrt{area}_{inc,\,max}$ in steel C. In steel A and D, the crack initiates from oxide inclusion, the inclusion at the fracture origin was debonded from matrix and remained on one side of fracture surface, or broke into two pieces on the same plane of fracture surface and remained on both side of fracture surface. In steel B and C, the crack initiates from MnS, the inclusion was broke into two pieces on the plane parallel to the specimen axis and remained on both side of fracture surface. The rough granular fracture

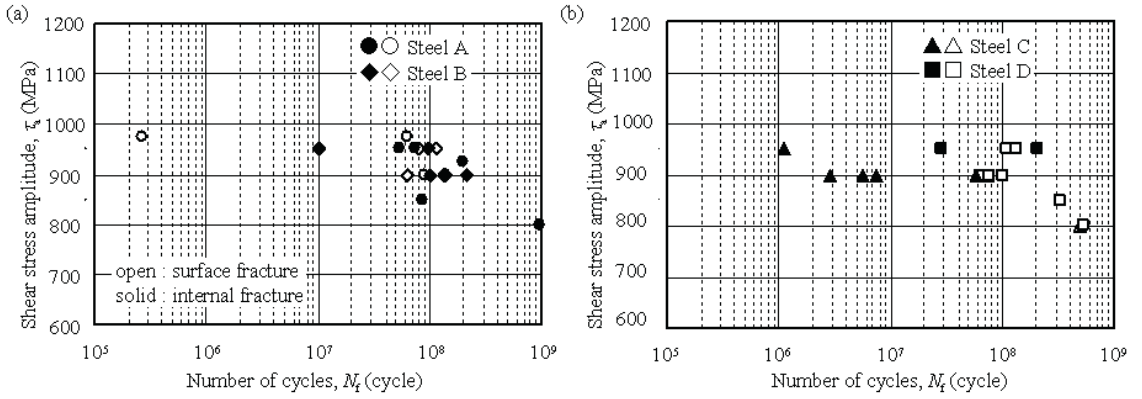

Fig. 2 S-N curves of ultrasonic torsional fatigue test.

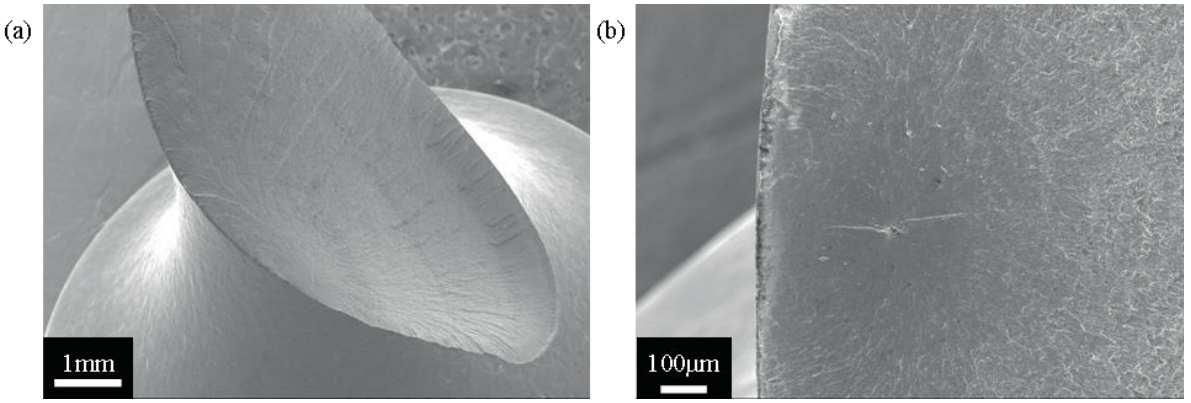

Fig. 3 Internal fracture specimen of steel A (τ_a=950MPa, N_f =5.4×10^{7}cycles) (a) over view; (b) fracture surface.

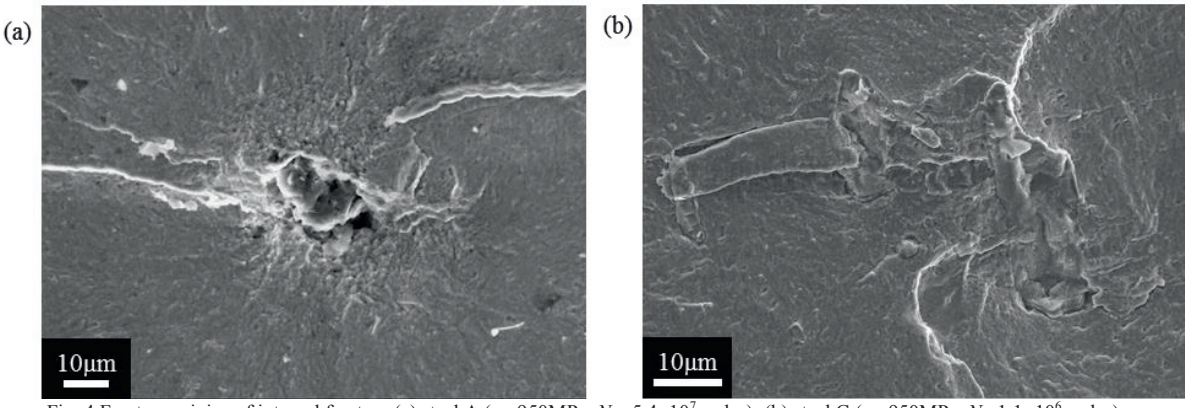

Fig. 4 Fracture origins of internal fracture (a) steel A (τ_a=950MPa, N_f =5.4×10^{7}cycles); (b) steel C (τ_a=950MPa, N_f=1.1×10^{6}cycles).

surface was found surrounding fracture origin in every inclusion at fracture origin. It was observed as a dark area by optical microscope, so the dark area is considered as an ODA. When a crack propagates in shear mode, the fracture surface should be smooth by ablation due to shear motion. Therefore the formation of ODA means that the crack propagates in tension mode.

3.3. Cross-section observation

As a result of fracture surface observation, it seems that the crack initiation behaviors are different between oxide inclusion and MnS. To consider the crack initiation behavior, the cross-section of fracture origin was bared by polishing and observed by SEM. Fig. 5 shows the SEM images of cross-section of fracture origin in steel A and C. Some part of inclusion was lost while polishing. In steel A, the crack initiated from $CaO\text{-}Al_2O_3$ complex inclusion, the fracture surface was formed an angle of about 45 degrees to the specimen axis, so the crack propagated in a mode I manner. In steel C, the fracture surface was formed also an angle of about 45 degrees to specimen axis and the crack was found in MnS in addition. The crack in MnS propagated to the direction of specimen axis which is parallel to the direction of maximum shear stress. So when the crack initiates from MnS, it propagates in shear mode at first, then it branched and propagated in a mode I manner. In the case of internal fracture under tension-compression stress, a crack propagates only in a mode I manner. But under shear stress, the crack propagation behavior is strongly affected by inclusion type.

4. Discussion

Fig. 6 shows the sketch of the crack initiation and propagation behavior under cyclic shear stress. On torsional

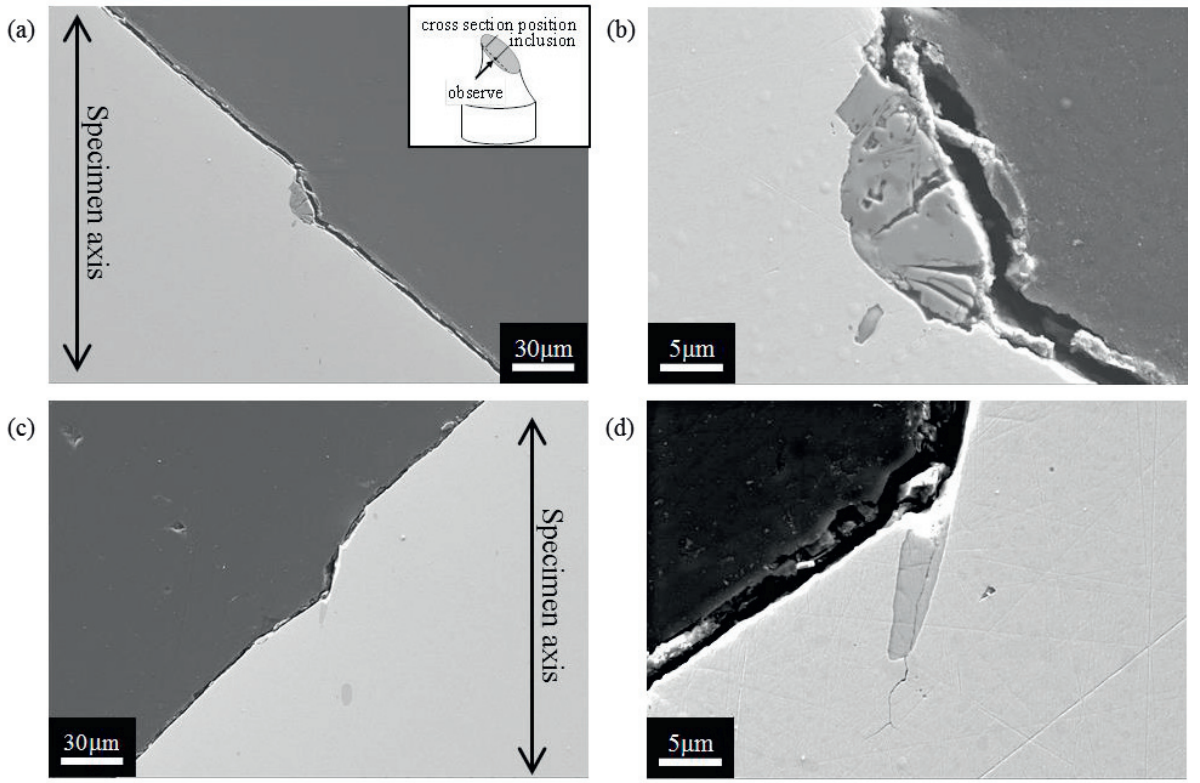

Fig. 5 Cross-section of fracture origin (a) and (b) steel A (τ_a=950MPa, N_f =5.4×10^{7}cycles); (c) and (d) steel C (τ_a=950MPa, N_f=1.1×10^{6}cycles).

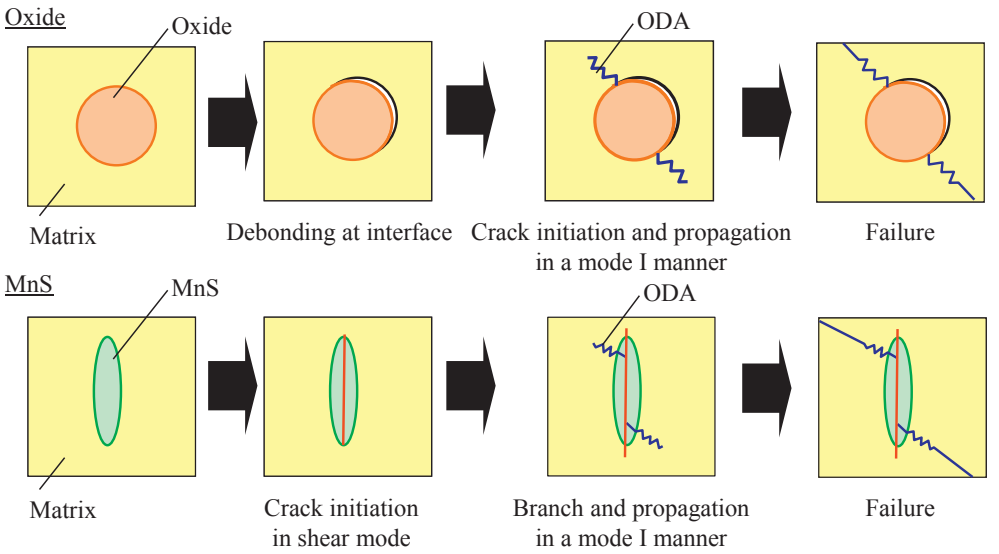

Fig. 6 Sketch of the crack initiation and propagation behaviour under cyclic shear stress.

fatigue test, in generally, the crack initiates and propagates in shear mode at first, then it branches and propagates in a mode I manner [11] [12]. But the oxide type inclusion such as Al_2O_3 is easy to debond from matrix interface [4], and shear stress is not applied on the matrix interface. The debonded surface was also found in Fig. 5. Therefore the crack initiates and propagates in a mode I manner. On the other hand, the easiness of debonding on MnS is not reported but obvious debonding was not found in cross-section observation shown in Fig. 5. Thus the crack initiates from MnS, which is softer than matrix, and propagates in shear mode at first, then it branches and propagates in a mode I manner. In either case, ODA is formed surrounding inclusion in tension mode. Consequently, the crack initiation and propagation behaviours are different on inclusion types under cyclic shear stress, so it is supposed that the characteristic of inclusion gives influences on fatigue properties. Furthermore, the crack initiation and propagation behaviour under shear stress is obviously different from the behaviour under tension-compression stress, so the fatigue properties of the materials which applied shear stress should be evaluated by torsional fatigue test.

5. Conclusions

Four kinds of high carbon chromium steel were conducted to ultrasonic torsional fatigue test and the fracture surfaces and the cross-sections of fracture origin were observed. The results are summarized as follows:

- Internal fatigue fracture was occurred from MnS and oxide inclusion, the ODA was found surrounding the inclusion.
- In the case that the crack initiates from oxide inclusion, it propagates in a mode I manner. When the crack initiates from MnS, it initiates and propagates in shear mode at first, then branches and propagates in a mode I manner.
- The characteristics of the inclusion, such as the shape, hardness or the state of bonding with matrix, influence to the crack initiation and propagation behaviors under cyclic shear stress.

Acknowledgement

This study was carried out as a part of research activities of “Fundamental Studies on Technologies for Steel Materials with Enhanced Strength and Functions” by Consortium of JRCM (The Japan Research and Development Center for Metals). Financial support from NEDO (New Energy and Industrial Technology Development Organization) is greatly acknowledged.

References

[1]Murakami Y, Nomoto T, Ueda T. Factors influencing the mechanism of superlong fatigue failure in steels. *Fatigue Fract Engng Mater Struct* 1999; 22, 581-590.

[2]Tanaka K, Akiniwa Y. Fatigue crack propagation behavior derived from S-N data in very high cycle regime. *Fatigue Fratct. Engng. Mater. Struct* 2002; 25, 775-784.

[3]Bathias C. There is no infinite fatigue life in metallic materials. *Fatigue Fract. Engng. Mater. Struct* 1999; 22, 559-565.

[4]Mayer H. Very high cycle fatigue properties of bainitic high carbon-chromium steel. *Int. J. Fatigue* 2009; 31, 242-249.

[5]Shiozawa K, Lu L, Ishihara S. S–N curve characteristics and subsurface crack initiation behavior in ultra-long life fatigue of a high carbon-chromium bearing steel. *Fatigue Fract. Engng. Mater. Struct* 2001; 24, 781-790

[6]Sakai T, Sato Y, Oguma N. Characteristic S–N properties of high-carbon-chromium-bearing steel under axial loading in long-life fatigue. *Fatigue Fract. Engng. Mater. Struct* 2002; 25, 765-773.

[7]Ishida W, Yamamoto T, Kaneda S, Ogawa T. Fatigue strength and internal crack growth behavior of high strength steel under variable amplitude stressing in very high cycle regime. *Trans. J. Soc. Mech. Eng* 2012; A 78, 23-33.

[8]Fufuya Y, Hirukawa H, Kimura T, Hayaishi M. Gigacycle Fatigue Properties of High-Strength Steels According to Inclusion and ODA Sizes. *Metall. Mater. Trans*. 2007; A 38, 1722-1730.

[9]Stanzl-Tschegg S E, Mayer H R, Tschegg E K. High frequency method for torsion fatigue testing. *Ultrasonics* 1993; 31, 275-280.

[10]Xue H Q, Bathias C. Crack path in torsion loading in very high cycle fatigue regime. *Eng. Fract. Mech.* 2010; 77, 1866-1873.

[11]Shimamura Y, Narita K, Ishii H, Tohgo K, Fujii T, Yagasaki T, Harada M. 2014. Fatigue properties of carburized alloy steel in very high cycle regime under torsional loading. *Int. J. Fatigue* 2014; 60, 57-62.

[12]Akiniwa Y, Stanzl-Tschegg S, Mayer H, Wakita M, Tanaka K, Fatigue strength of spring steel under axial and torsional loading in the very high cycle regime. *Int. J. Fatigue* 2008; 30, 2057-2063.